Catalysis Today 176 (2011) 36–40

Contents lists available at ScienceDirect

Catalysis Today

journal homepage: www.elsevier.com/locate/cattod

Catalytic combustion of methane over mesoporous silica supported palladium

Joelle Bassil[a], Abdulkader AlBarazi[b], Patrick Da Costa[b], Maya Boutros[a,*]

[a] Université Libanaise, Faculté des sciences II, Laboratoire de Chimie Physique des Matériaux (LCPM), Campus Fanar, BP 90656, Jdeideh, Lebanon
[b] Université Pierre et Marie Curie, UPMC Paris 6, Institut Jean Le rond d'Alembert (UMR 7910), 2 place de la gare de ceinture, 78210 Saint Cyr l'ecole, France

ARTICLE INFO

Article history:
Received 30 September 2010
Received in revised form 19 April 2011
Accepted 27 May 2011
Available online 20 July 2011

Keywords:
Mesoporous silica
SBA-15
Palladium, SCR NO_x
Methane oxidation

ABSTRACT

Pd nanoparticles with controlled size have been prepared by nanocasting of a mesoporous silica SBA-15. Two methods of impregnation were tested: incipient wetness impregnation and ion exchange. Pd was ion-exchanged with the silanol groups on non-calcined silica, prepared by solvent extraction of the template. The structural and porosity properties of these materials were studied by XRD, N_2 sorption and TEM imaging. The nature of palladium species in these catalysts were investigated by UV–vis, TEM and high angle XRD. Whatever the method of impregnation, the particles of palladium are very small and well dispersed on the surface of support. The solids were tested in the catalytic combustion of methane and in the selective catalytic reduction of NO_x with methane. The activity of both catalysts for this last reaction is very low. For methane catalytic combustion, these Pd/mesoporous materials demonstrate higher conversions and the Pd-SBA-15 sample prepared by ion exchange showed a light of temperature (T50) 75 °C lower than the one exhibited by the sample prepared by incipient wetness impregnation.

1. Introduction

Catalytic combustion of methane has received considerable attention in the last decades due to its practical applications in both power generation and pollutant abatement [1,2]. This reaction has been shown to be effective in producing energy in gas turbine combustors. Compared to the conventional thermal combustion process, using a heterogeneous catalyst can remarkably decrease the reaction temperature, thereby reducing the noxious emissions of nitrogen oxides [3,4]. The abundance of methane makes the SCR of NO_x by methane a promising and attractive technology for the abatement of NO_x emissions from stationary sources [5]. Much of the CH_4-SCR research has examined precious metal catalysts such as Pt, Pd and Rh [6–8] to compare their relative performance with respect to each other and with respect to other metal oxides catalysts such as Co, Fe, or Cu [9] but in general the activity of noble metals is higher than that of metal oxides. Several ion-impregnated zeolitic catalysts (Mn, Ni, Pd, Co, etc.) for CH_4-SCR were tested under oxidizing conditions. CuPd is a potential catalyst for NO reduction with methane [10]. Zeolite ZSM-5 provides well-dispersed ion exchange sites, but the support does not give a uniquely low temperature for methane activation or efficient CH_4-SCR [10].

Pd-based catalysts are renowned for their excellent activity in methane combustion under lean conditions and have been extensively studied in recent years [11–13]. Due to its high methane combustion values Pd is a widely used noble metal in the three-way catalyst (TWC) formulation, however, its catalytic activity can be controlled by the synthesis method employed [14]. Thus, Pd catalysts may vary from being inactive to very active depending on the catalysts design [15]. Amongst the most investigated issues affecting methane combustion, the nature of the active sites, Pd oxidation state, the effects of particle size and the nature of the supports can be easily pointed out as the more relevant ones [16,17]. Therefore, different oxides, such as silica and zirconia, and even some types of zeolites, have been employed in the preparation of supported palladium systems [18–20].

Recently developed mesoporous silicates such as SBA and MCM family due to their unique properties have shown to be suitable supports for metal and metal oxide nanoparticles. These mesoporous molecular sieves possess high specific surface area, large specific pore volume and highly ordered pore structure with narrow size distribution.

The metals were introduced into the support either directly during the mesoporous silicate synthesis or by post-synthesis treatment. The addition of a metal precursor into the synthesis gel leads to the uncontrolled growth of metal particles inside the pores and on the external support surface, resulting in a broad particle size distribution [21]. The post-synthesis metal deposition was carried out using a calcined mesoporous support via incipient wetness impregnation [22], ion-exchange [23], equilibrium adsorption, metal complex immobilization [24] and vapor phase grafting [25].

Recently, mesoporous silica supported noble metal catalysts have been successfully applied in the removal of emissions of

* Corresponding author. Tel.: +961 71 349 766; fax: +961 1 681 552.
E-mail addresses: Patrick.da_costa@upmc.fr (P. Da Costa), boutrosmaya@hotmail.com (M. Boutros).

0920-5861/$ – see front matter © 2011 Elsevier B.V. All rights reserved.
doi:10.1016/j.cattod.2011.05.026

volatile organic compounds as well as in the selective catalytic reduction of NO_x by methane [26]. The catalytic performance of palladium catalysts in methane combustion with the ordered mesoporous molecular sieve Al-MCM-41 and MCM-41 as the model support were recently studied [27–29]. However, there is no systematic investigation of the use of SBA-15 mesoporous molecular sieves as support for the catalytic combustion of methane or for CH_4-SCR of NO_x.

The aim of our paper is to reach a better dispersion of the palladium particles on SBA-15 mesoporous silica. We investigate the influence of the impregnation method on the physico-chemical properties, the morphology of palladium nanoparticles and the catalytic performances of mesoporous supported palladium catalysts in methane oxidation and NO_x reduction by CH_4.

2. Experimental

Two types of Pd/mesoporous silica were synthesized using two methods of impregnation: incipient wetness impregnation (IWI) and ion exchange (IE). These solids were characterized by X-ray diffraction, N_2 sorption, transmission electronic microscopy (TEM), and UV–vis. The catalytic performances of these solids were studied in the combustion of methane and the reduction of NO_x using CH_4 as reducing agent.

2.1. Catalysts synthesis

(a) Pure silica SBA-15 prepared using Pluronic-123: $EO_{20}PO_{70}EO_{20}$ as a templating agent was synthesized according to the method described by Zhao et al. [30]. The template was removed by calcination under air flow at 550 °C or by Soxhlet extraction with ethanol for 48 h.
(b) The catalyst *Pd-SBA-15* (*IWI*) was prepared by incipient wetness impregnation of the calcined SBA-15 support. The palladium precursor used is tetramine palladium(II) nitrate $Pd(NH_3)_4(NO_3)_2$. The palladium containing aqueous solution (1.1 mL) is added to 1 g of SBA-15 support.
(c) Palladium was introduced into the synthesized mesoporous silicas via ion-exchange from $Pd(NH_3)_4(NO_3)_2$ aqueous solution. The mesoporous silicas prepared by solvent extraction of the template were commonly used for the Pd clusters formation [21].

In a typical synthesis, the amount of $Pd(NH_3)_4(NO_3)_2$ corresponding to a selected Pd loading was dissolved in 40 mL of H_2O. Ammonium hydroxide (10 wt%) was added to reach pH ~ 8. Mesoporous silica (1 g) was introduced in the prepared ion-exchange solution, and the mixture was stirred vigorously at room temperature for 4 h. The resulting solid (*Pd-SBA-15* (*IE*)) was filtered out, washed carefully with water and air-dried over night.

The theoretical loading of palladium introduced is 0.5 wt% in the (b) and (c) cases. The desired catalysts Pd-SBA-15 were calcined under air flow at 500 °C for 2 h.

2.2. Catalyst characterization

Palladium and silicon composition of the various materials were determined by fluorescence X on a "Spectro XEPOS".

The calcined samples were evaluated by powder X-ray diffraction using a Bruker D8 Advance X-ray diffractometer at Cu Kα radiation (λ = 0.15418 nm). The specific surface area, pore volume and pore diameter of all calcined samples were determined from N_2 sorption data obtained at 77 K using an ASAP 2010 micromeritics instrument. Prior to the analysis, the samples were outgassed at 200 °C until a stable static vacuum of 2×10^{-3} Torr was reached. The pore diameter and specific pore volume were calculated according to the BJH model. The specific surface area was obtained by using the BET equation.

Transmission electron analyses were performed on a JEOL-JEM 2011 HR (LaB) microscope operating at 200 kV. The powdered samples were dispersed in ethanol and the resulting suspensions deposited on a copper grid coated with a porous carbon film.

EDS analysis was performed with the same apparatus using a LINK AN 10,000 system, connected to a silicon–lithium diode detector, and multichannel analyser.

Diffuse reflectance spectra were recorded at room temperature between 190 and 2500 nm on a Varian Cary 5E spectrometer equipped with a double monochromator and an integrating sphere coated with polytetrafluoroethylene (PTFE) as reference.

2.3. Catalytic measurements

Temperature-programmed surface reaction (TPSR) and steady state experiments were carried, in a U-type glass reactor by using gas mixture consisting of 150 ppm NO + 1500 ppm CH_4 + 7% O_2 in Ar. The gases (NO, O_2 and Ar) were fed from compressed cylinders provided by Air Liquide and adjusted with Brooks mass flow controllers (5850 TR and 5850 TE). For all experiments, the total flow rate of the feed gas was maintained at 250 mL min^{-1}. The sample (90 mg) was held on plugs of quartz wool and the temperature was controlled through a EUROTHERM 2408 temperature controller, K-type thermocouple. The gas hourly space velocity (GHSV) was 22,100 h^{-1}. The outflow experimental reaction was continuously monitored a variety of detectors such as An Eco Physics CLD 700 AL chemiluminescence NO_x analyser (for NO and total NO_x (i.e. NO + NO_2), which allowed the simultaneous detection of NO and NO_x. Two Ultramat 6 IR analysers were used to monitor N_2O, CO and CO_2. A FID detector (Fidamat 5) was used to follow the concentration of the hydrocarbonated compounds.

3. Results and discussion

3.1. Characterization of the support and active phase

In order to obtain a high concentration of silanol groups on the mesopore surface, before ion exchange the template of SBA-15 support was removed by solvent extraction [31].

The ion exchange of silanol groups with precursor cations is the common technique used for the metal deposition on the internal wall surface of the mesopores [21]. It was mentioned in the literature that the pH value of the aqueous solution of $[Pd(NH_3)_4]^{2+}$ would affect the Pd content introduced into SBA-15 by the adsorption method. No Pd could be incorporated into SBA-15 if the pH value was kept below 8 [32].

In our case, the palladium content of the solid obtaind by ion exchange is 0.25 wt%, we can demonstrate that 50% of Pd was incorporated which is in agreement with the litterature (40% at pH 8.3 [32]). This value is slightly higher than that obtained in the case of Pd-SBA-15 (IWI) (0.18 wt%, 36%).

The structure and the mesoporosity of the different solids were determined by their low-angle XRD patterns and N_2 sorption isotherms, respectively.

Compared to the pure calcined silica SBA-15, Fig. 1 shows that Pd-SBA-15 (IWI) has three well-resolved characteristic diffraction peaks which are attributed to 1 0 0, 1 1 0 and 2 0 0 of hexagonal structure. In the case of Pd-SBA-15 (IE), (Fig. 1 curve c), a gradual decrease of the intensities of each peak is observed. The reflections corresponding to the (1 1 0) and (2 0 0) planes cannot be easily discerned indicating that it is much less structured than other samples.

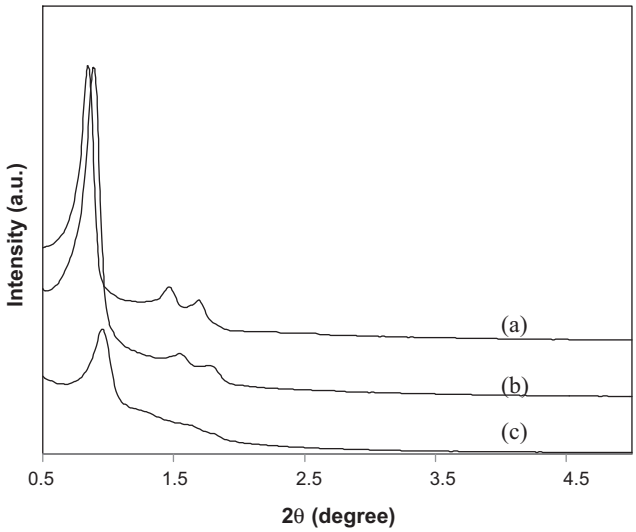

Fig. 1. X-ray diffraction patterns of (a) SBA-15, (b) Pd-SBA-15 (IWI) and (c) Pd-SBA-15 (IE).

Table 1
Structural parameters of SBA-15 and Pd-SBA-15 samples.

Samples	θ (°)	d_{100}[a] (Å)	a[b] (Å)
Si-SBA-15	0.42	105.17	121.44
Pd-SBA-15 (IWI)	0.44	100.39	115.92
Pd-SBA-15 (IE)	0.48	92.02	106.26

[a] $d_{100} = \lambda/2 \sin\theta$.
[b] $a = 2d_{100}/\sqrt{3}$.

According with the literature, the use of alkaline medium for adsorption may affect the long-range regularity of mesoporous array of Pd-SBA-15 (IE) sample [32,33].

It was noticed that the diffraction peaks of palladium containing mesoporous silica, are less shifted to higher values than those of pure SBA-15 silica related to a decrease of structural parameters (d_{hkl} and a_0, Table 1). This difference is maybe related to the presence of Pd particles inside the mesopores channels of SBA-15 support.

N_2 adsorption–desorption isotherms of calcined SBA-15 support and Pd-SBA-15 samples exhibit characteristic type IV isotherms with a H1 hysteresis loop as defined by IUPAC (Fig. 2). The steep increases of the adsorption volume at P/P_0 (0.6–0.8) are due to capillary condensation of nitrogen in the mesopores. The inset of

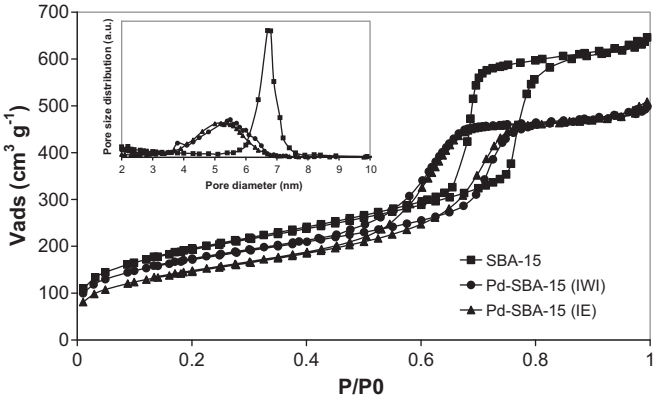

Fig. 2. N_2 adsorption–desorption isotherms at 77 K of SBA-15, Pd-SBA-15 (IWI) and Pd-SBA-15 (IE) [inset: pore size distribution curves of SBA-15 and Pd-SBA-15 samples].

Table 2
Physico-chemical properties of SBA-15 and Pd-SBA-15 samples.

Samples	Si (wt%)	Pd (wt%)	S_{BET} ($m^2\ g^{-1}$)	V_{pores} ($cm^3\ g^{-1}$)	D_{pores} (nm)
Si-SBA-15	–	–	800	1.15	6.7
Pd-SBA-15 (IWI)	48	0.18	665	0.85	5.5
Pd-SBA-15 (IE)	48	0.25	525	0.75	5.2

Fig. 2 shows a typical BJH pore size distribution for SBA-15 and the palladium containing mesoporous materials. The presence of palladium leads to a decrease in the pore diameters from 6.7 nm (SBA-15) to 5.5 nm and 5.2 nm for Pd-SBA-15 (IWI) and pd-SBA-15 (IE), respectively.

The textural parameters of the Pd-SBA-15 samples prepared with two different methods of impregnation are listed in Table 2. The inclusion of palladium by ion exchange into the structure of SBA-15 conducted to a large modification of the specific surface area (−35%) that is not the case of Pd-SBA-15 (IWI) sample (−17%). The decrease of the BET surface area and pore volume is the result of the incorporation of the metal inside the mesopores channel of SBA-15. The strongly alkaline pH used in the ion exchange method could also affect the S_{BET} of the Pd-SBA-15 (IE) sample.

TEM images of Pd-SBA-15 samples indicate that these solids are well mesostructured despite the introduction of metal on the support (Fig. 3). Dispersed palladium nanoparticles are mainly located

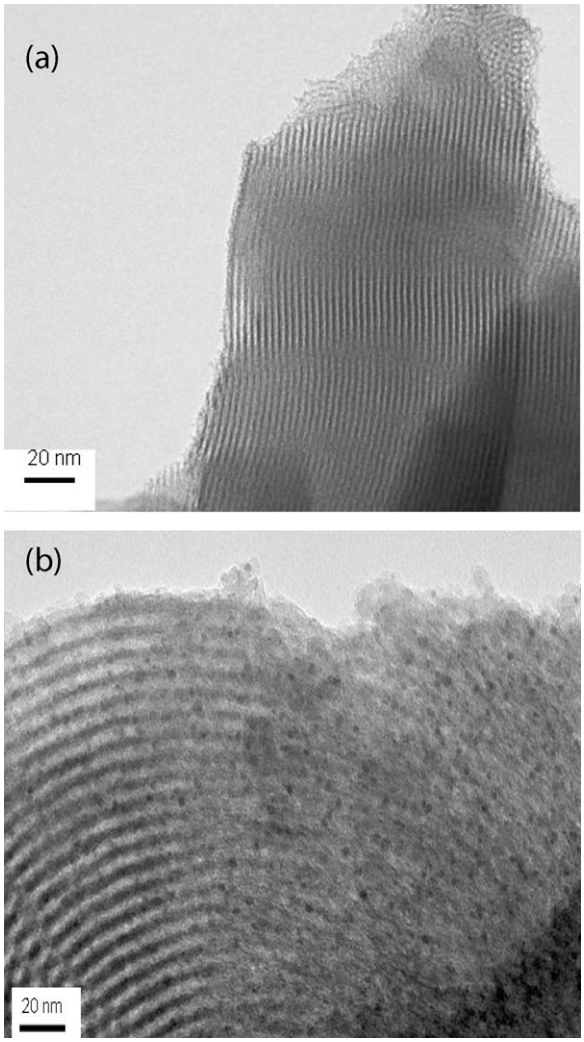

Fig. 3. TEM images of (a) Pd-SBA-15 (IWI) and (b) Pd-SBA-15 (IE).

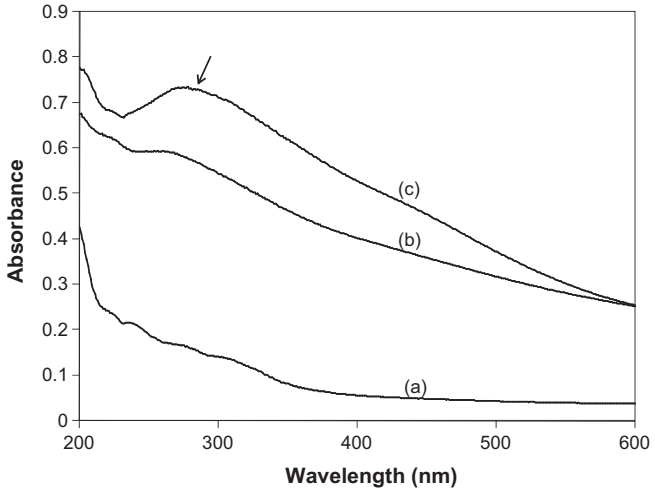

Fig. 4. Diffuse reflectance UV–vis spectra of (a) SBA-15, (b) Pd-SBA-15 (IWI) and (c) Pd-SBA-15 (IE).

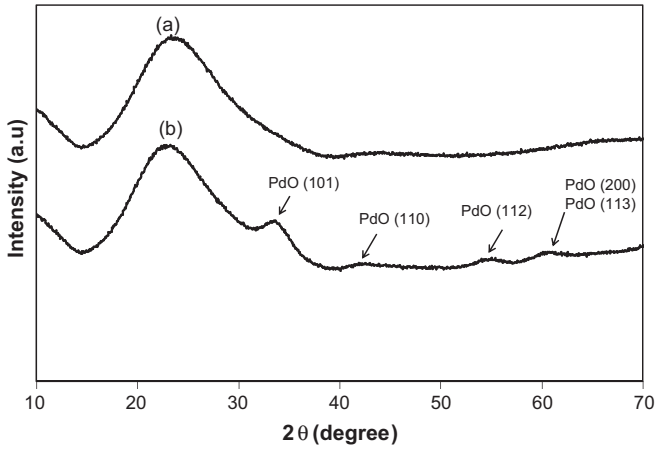

Fig. 5. High angle X-ray diffraction patterns of (a) Pd-SBA-15 (IWI) and (b) Pd-SBA-15 (IE).

inside the pore channels in the case of Pd-SBA-15 (IE). Their average size (3–4 nm) is smaller than the pore aperture. The presence of silicon and palladium was detected by EDS; this lack of visibility confirms the good dispersion of palladium particles upon the support.

For Pd-SBA-15 (IWI), no particles corresponding to palladium are detected by TEM (Fig. 3(a)), although EDS showed Pd/Si ratios are constant. Palladium species are then highly dispersed on the support with a diameter much smaller than the pores of SBA-15 solid.

The UV–vis diffuse reflectance was performed to characterize the palladium species. As shown in Fig. 4, a band at ~280 nm was observed for the Pd containing mesoporous silica could be ascribed to highly dispersed Pd(II)O clusters or small PdO particles [33]. The intensity of this band increase when the amount of Pd increases (case of Pd-SBA-15 (IE)).

An absorption in the UV range at 210 nm was slightly detected for Pd mesoporous silica materials, which is in good agreement with reported values [34]. This band could be attributed to the $d\pi$–$p\pi$ charge transfer transition between Pd and oxygen of small PdO particles. No band characteristic of Pd^{2+} species (~400 nm) was detected [35]. One can conclude that the Pd(II) species attached on silica wall of SBA-15 were transformed to Pd(II)O clusters or PdO small nanoparticles after calcination of our Pd-SBA-15 samples under air flow at 550 °C.

The high angle XRD patterns of the calcined Pd/mesoporous silica shows a broad peak about $2\theta = 22°$ ascribed to the amorphous silica (Fig. 5). In the case of Pd-SBA-15 (IE) sample, another peak at 33.8° was detected which corresponding to the PdO (1 0 1) reflection [36]. The reflections for PdO (1 1 0), (1 1 2), (2 0 0) and (1 1 3) were slightly observed (Fig. 5(b)). This small amount of PdO was detected despite the low percentage of metal introduced, and could be related to some aggregates created after calcination on the external surface of Pd/mesoporous silica. However, for the sample prepared by incipient wetness impregnation (Pd-SBA-15 (IWI)), the detection of PdO phase by X-ray was difficult. This may be related to the presence of small particles of PdO highly dispersed on the surface of support and it was hardly observed by TEM.

3.2. Pd-SBA-15 catalytic activity

The catalysts performance of Pd/mesoporous silica was evaluated by their global activity in methane combustion. Hence the development of methane conversion was monitored as a function of temperature (Fig. 6).

The methane combustion started at about 300 °C; then the conversion into CO and CO_2 increased drastically with the reaction temperature and the complete conversion was reached at 400 °C and 500 °C for Pd-SBA-15 (IE) and Pd-SBA-15 (IWI) respectively. The catalytic activity of Pd-SBA-15 was affected by the preparation procedure. In comparison, the Pd-SBA-15 (IE) remains more active at low temperature than SBA-15 and Pd-SBA-15 (IWI). We can conclude that the Pd-SBA-15 (IE) showed a light of temperature (T50) 75 °C lower than the one exhibited by the sample prepared by incipient wetness impregnation.

It has been pointed out in the literature that the activity of Pd based catalysts in methane combustion depends strongly on the surface acidity [37], the size of PdO crystallites [38], and the Pd oxidation state [39]. In our case, the good reactivity of our Pd based catalysts samples can be attributed to the presence of well dispersed PdO nanoparticles on the surface of SBA-15 support. According to the literature, the good dispersion of PdO nanoparticles, giving an intimate contact with the support, leads to a good activity for the oxidation reaction [27]. The smaller particles, obtained in our samples, are easier to oxidize and to form an active PdO layer than the larger particles. The Pd particle size does play an important role in the combustion of methane: small particles (less than 1–2 nm) seem to provide early ignition; medium size (4–10 nm) crystallites are likely to increase the reaction rate; while large particles (about 100 nm) do not further improve the activity [40]. It seems that an optimal particle size exists [40]. In

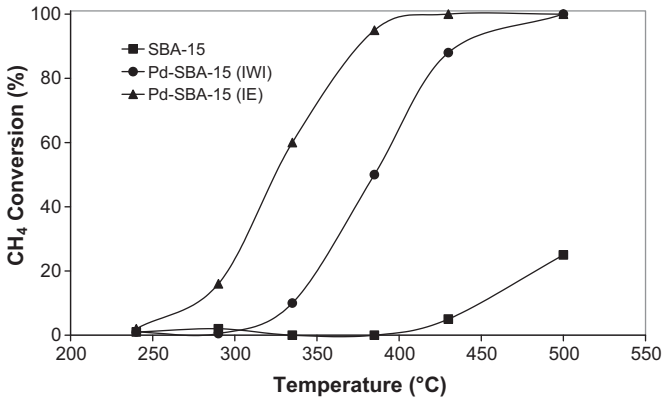

Fig. 6. Steady-state methane conversion as function of temperature for SBA-15 and Pd-SBA-15 samples.

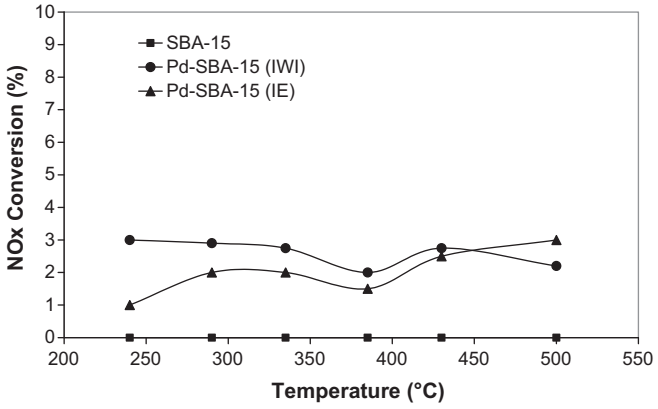

Fig. 7. Steady state NO_x conversion as function of temperature for SBA-15 and Pd-SBA-15 samples.

our case, the small difference between the two samples Pd-SBA-15 (IE) and Pd-SBA-15 (IWI) can be related to the percentage of Pd slightly greater in the case of Pd-SBA-15 (IE). The PdO particle size of about 4 nm detected in Pd-SBA-15 (IE) increases the rate of reaction at low temperature in comparison with the smaller particles (<2 nm) observed in the sample Pd-SBA-15 (IWI). The improved stability observed on the Pd-SBA-15 catalysts was closely related to the stronger interaction between palladium oxide and molecular sieve support.

The reduction conversion of NO_x by CH_4 as reducing agent NO_x as function of temperature is presented in Fig. 7. In all experiments, no N_2O was detected and only nitrogen was observed as product. Whatever the method of impregnation of SBA-15 by $Pd(NH_3)_4(NO_2)_2$, the palladium catalysts prepared on the mesoporous silica have a lower activity for the reduction of NO_x by CH_4. The Pd-SBA-15 solids had a maximum NO conversion less than 4%. Despite the highly dispersed and small size of PdO nanoparticles, the low activity of these samples could be attributed to different factors such as the low acidity of the support or the limited percentage of Pd incorporated ~0.2%.

4. Conclusion

Synthesis of Pd-nanoparticles in mesoporous silica was performed using two methods of impregnation: incipient wetness and ion exchange. The palladium nanoparticles obtained were located inside the mesoporous channels of SBA-15. The average size of the nanoparticles is smaller than the pore diameter aperture.

A decrease of textural and structural parameters was observed showing the incorporation of palladium in the channels of SBA-15 solids. The variation of the support properties could be attributed to the strongly alkaline pH used in the ion exchange method. Small PdO nanoparticles and Pd(II)O clusters species were detected by UV–vis and XRD high angles.

In the presence of Pd based mesoporous silica, the oxidation of methane is complete at a temperature ≥400 °C. In the presence of NO_x, a lower light off temperature is observed for Pd-SBA-15 prepared by ion exchange method.

Acknowledgments

The authors thank Dr. Thomas Onfroy for N_2 sorption measurements and Sandra Casale for TEM analysis.

References

[1] E. Tzimpilis, N. Moschoudis, M. Stoukides, P. Bekiaroglou, Appl. Catal. B 84 (2008) 607.
[2] Q. Liu, A.Q. Wang, X.H. Wang, P. Gao, X.D. Wang, T. Zhang, Micropor. Mesopor. Mater. 111 (2008) 323.
[3] J.G. McCarty, Nature 403 (2000) 35.
[4] V. Dupont, S.-H. Zhang, R. Bentley, A. Williams, Fuel 81 (2002) 799.
[5] R. Marques, L. Mazri, S. Da Costa, F. Delacroix, G. Djega-Mariadassou, P. Da Costa, Catal. Today 137 (2008) 179.
[6] A. Wang, D. Liang, C. Xu, X. Sun, T. Zhang, Appl. Catal. B 32 (2001) 205.
[7] H. Ohtsuka, T. Tabata, Appl. Catal. B 29 (2001) 177.
[8] H. Hamada, Y. Kintaichi, M. Sakai, T. Ito, M. Tabata, Appl. Catal. 75 (1991) L1.
[9] R. Burch, A. Ramli, Appl. Catal. B 15 (1998) 49.
[10] L.O. Öhman, B. Ganemi, E. Björnbom, K. Rahkamaa, R.L. Keiski, J. Paul, Mater. Chem. Phys. 73 (2002) 263.
[11] C.-B. Wang, C.-M. Ho, H.-K. Lin, H.-C. Chiu, Fuel 81 (2002) 1883.
[12] B. Stasinska, A. Machocki, K. Antoniak, M. Rotko, J.L. Figueiredo, F. Gonçalves, Catal. Today 137 (2008) 329.
[13] Y.-X. Pan, C.-J. Liu, P. Shi, Appl. Surf. Sci. 254 (2008) 5587.
[14] J.C. Martin, S. Suarez, M. Yates, P. Ávila, Chem. Eng. J. 150 (2009) 8.
[15] C.J. Loughran, D.E. Resasco, Appl. Catal. B 7 (1995) 113.
[16] M. Lyubovsky, L. Pfefferle, Catal. Today 47 (1999) 29.
[17] Y. Ozawa, Y. Tochihara, A. Watanabe, M. Nagai, S. Omi, Appl. Catal. A 258 (2004) 261.
[18] K. Fujimoto, F. Ribeiro, M. Avalos-Borja, E. Iglesia, J. Catal. 179 (1998) 431.
[19] I. Yuranov, P. Moeckli, E. Suvorova, P. Buffat, L. Kiwi-Minsker, A. Renken, J. Mol. Catal. A 192 (2003) 239.
[20] K. Okumura, S. Matsumoto, N. Nishiaki, M. Niwa, Appl. Catal. B 40 (2003) 151.
[21] I. Yuranov, P. Moeckli, E. Suvorova, P. Buffat, L. Kiwi-Minsker, A. Renken, J. Mol. Catal. A: Chem. 192 (2003) 239.
[22] M. Boutros, J.M. Trichard, P. Da Costa, Top. Catal. 52 (2009) 1781.
[23] P. Magnoux, N. Lavaud, M. Guisnet, Top. Catal. 13 (2000) 291.
[24] A. Fukuoka, N. Higashimoto, Y. Sakamoto, M. Sasaki, N. Sugimoto, S. Inagaki, Y. Fukushima, M. Ichikawa, Catal. Today 66 (2001) 23.
[25] K.B. Lee, S.M. Lee, J. Cheon, Adv. Mater. 13 (2001) 517.
[26] J.M.D. Coĩnsul, C.A. Peralta, E.V. Benvenutti, J.A.C. Ruiz, H.O. Pastore, I.M. Baibich, J. Mol. Catal. A 246 (2006) 33.
[27] Z.-J. Wang, Y. Liu, P. Shi, C.-J. Liu, Y. Liu, Appl. Catal. B: Environ. 90 (2009) 570.
[28] J.A.C. Ruiz, M.A. Fraga, H.O. Pastore, Appl. Catal. B: Environ. 76 (2007) 115.
[29] A.M. Venezia, R. Murania, G. Pantaleo, G. Deganello, J. Catal. 251 (2007) 94.
[30] D. Zhao, Q. Huo, J. Feng, F. Chmelka, G.D. Stucky, J. Am. Chem. Soc. 120 (1998) 6024.
[31] L. Mercier, T.J. Pinnavaia, Environ. Sci. Technol. 32 (1998) 2749.
[32] N. Yao, C. Pinckney, S. Lim, C. Pak, G.L. Haller, Micropor. Mesopor. Mater. 44–45 (2001) 377.
[33] C. Li, Q. Zhang, Y. Wang, H. Wan, Catal. Lett. 120 (2008) 126.
[34] W. Chen, J. Zhang, W. Cai, Scripta Mater. 48 (2003) 1061.
[35] R. Marques, S. Capela, S. Da Costa, F. Delacroix, G. Djega-Mariadassou, P. Da Costa, Catal. Commun. 9 (2008) 1704.
[36] S.-S. Lee, H.-I. Park, B.-K. Park, S.-H. Byeon, Mater. Sci. Eng. B 135 (2006) 20.
[37] L.M.T. Simplıĩcio, S.T. Brandã̃o, E.A. Sales, L. Lietti, F. Bozon-Verduraz, Appl. Catal. B 63 (2006) 9.
[38] O. M'Ramadj, D. Li, X. Wang, B. Zhang, G. Lu, Catal. Commun. 8 (2007) 880.
[39] C. Shi, L. Yang, J. Cai, Fuel 86 (2007) 106.
[40] E. Pocoroba, L.J. Petersson, J. Agrell, M. Boutonnet, K. Jnasson, Top. Catal. 16/17 (2001) 407.